# Effect of chemical environment on the radiation chemistry of N , N -di-(2-ethylhexyl)butyramide (DEHBA) and plutonium retention

Gregory Horne, Christopher Zarzana, Travis Grimes, Cathy Rae, Joakim Ceder, Stephen Mezyk, Bruce Mincher, Marie-Christine Charbonnel, Philippe Guilbaud, George Saint-Louis, et al.

INL/JOU-19-53296-Revision-0

# Effect of Chemical Environment on the Radiation Chemistry of N,N-di-(2-ethylhexyl)butyramide (DEHBA) and Plutonium Retention

**Gregory P Horne, Christopher A Zarzana, Travis S Grimes, Cathy Rae, Joakim Ceder, Bruce J Mincher, Stephen P Mezyk, Marie-Christine Charbonnel, Laurence Berthon, Philippe Guilbaud, George Saint-Louis**

**September 2019**

**Idaho National Laboratory**
**Idaho Falls, Idaho 83415**

**http://www.inl.gov**

**Prepared for the**
**U.S. Department of Energy**

**Under DOE Idaho Operations Office**
**Contract DE-AC07-05ID14517**

# Effect of Chemical Environment on the Radiation Chemistry of *N*,*N*-di-(2-ethylhexyl)butyramide (DEHBA) and Plutonium Retention

Gregory P. Horne,*[a] Christopher A. Zarzana,*[a] Travis S. Grimes,[a] Cathy Rae,[a] Joakim Ceder,[a,b] Stephen P. Mezyk,[c] Bruce J. Mincher,[a] Marie-Christine Charbonnel,[d] Philippe Guilbaud,[d] George Saint-Louis,[d] and Laurence Berthon[d]

*N*,*N*-di-(2-ethylhexyl)butyramide (DEHBA) has been proposed as part of a hydro-reprocessing solvent extraction system for the co-extraction of uranium and plutonium from spent nuclear fuel, owing to its selectivity for hexavalent uranium and tetravalent plutonium. However, there is a critical lack of quantitative understanding regarding the impact of chemical environment on the radiation chemistry of DEHBA, and how this would affect process performance. Here we present a systematic investigation into the radiolytic degradation of DEHBA in a range of *n*-dodecane solvent system formulations, where we subject DEHBA to gamma irradiation, measure reaction kinetics, ligand integrity, degradation product formation, and investigate solvent system performance through uranium and plutonium extraction and strip distribution ratios. The rate of DEHBA degradation in *n*-dodecane was found to be slow ($G$ = -0.31 ± 0.02 μmol $J^{-1}$) but enhanced upon contact with the oxidizing conditions of the investigated solvent systems (organic-only, or in contact with either 0.1 or 3.0 M aqueous nitric acid). Two major degradation products were identified in the organic phase, *bis*-2-ethylhexylamine (b2EHA) and *N*-(2-ethylhexyl)butyramide (MEHBA), resulting from the cleavage of C–N bonds, and could account for the total loss of DEHBA up to ~300 kGy for organic-only conditions. Both b2EHA and MEHBA were also found to be susceptible to radiolytic degradation, having $G$-values of -0.12 ± 0.01 and -0.08 ± 0.01 μmol $J^{-1}$, respectively. Solvent extraction studies showed: (i) negligble change in uranium extraction and stripping with increasing absorbed; and (ii) plutonium extraction and retention exhibits complex dependencies on absorbed dose and chemical environment. Organic-only conditions afforded enhanced plutonium extraction and retention attributed to b2EHA, while acid contacts inhibited this effect and promoted significant plutonium retention for the highest acidity. Overall it has been demonstrated that chemical environment during irradiation has a significant influence on the extent of DEHBA degradation and plutonium retention.

## Introduction

Recycling (reprocessing) spent nuclear fuel (SNF) is key to maximizing energy content utility, environment stewardship, and continuing responsible nuclear waste management. The current industrial standard for reprocessing SNF is the Plutonium Uranium Redox EXtraction (PUREX) process, a solvent extraction technology that employs tributyl phosphate (TBP) to complex plutonium and uranium, facilitating their recovery from fission products and nuclear waste materials. However, TBP degrades to form undesirable products when subject to an intense multi-component radiation field under process conditions. To this end, extensive studies have been devoted to the development of alternative ligands to ultimately improve upon, and replace, TBP. Among the various reagents studied, the *N*,*N*-dialkyl monoamide class of ligands have demonstrated great potential due to their tuneable selectivity. Modifications can be easily made to either increase or decrease selectivity for a particular ion; e.g., selectivity for hexavalent versus tetravalent ions. A particularly promising TBP alternative is the monoamide, *N*,*N*-di-(2-ethylhexyl)butyramide (DEHBA, Fig. 1), which possesses a combination of alkyl chains and an *n*-alkane acyl group that facilitate efficient and selective extraction of hexavalent uranium and tetravalent plutonium under conditions typically employed by the PUREX process: a ligand-loaded organic phase in contact with aqueous nitric acid ($HNO_3$) containing dissolved SNF. Relative to TBP, the *N*,*N*-dialkyl monoamide class of ligands are characterized by greater selectivity for uranium over fission products, reputed higher radiolytic stability, and the generation of more benign radiolysis products, as summarized by Gasparini and Grossi.[1] Their improved radiolytic stability is particularly attractive, especially as the reprocessing of higher burn-up, mixed oxide (MOX) fuels becomes more common. Further, the monoamides can ultimately be incinerated, being composed entirely of carbon, hydrogen, oxygen, and nitrogen (CHON), which simplifies the waste treatment for used solvents. A current review by McCann *et al.* discusses the structural features of monoamides that favour selectivity and minimize third phase formation during actinide solvent extraction.[2]

SNF solvent extraction ligands must maintain their extraction and stripping efficiencies in the presence of an intense, multi-component radiation field. In this regard, the monoamides have previously been reported as exhibiting exceptional radiation stability.[3-5] A more recent investigation into the radiation stability of *di*-2-ethylhexylisobutryamide (DEH*i*BA) afforded radiolytic yields, $G$-values, of -0.53 μmol $J^{-1}$, slightly higher than those of TBP (-0.37 μmol $J^{-1}$).[6,7] Based on only these degradation rates, both ligands would be suitable for SNF reprocessing applications.[8] However, an additional requirement for process suitability is that ligand degradation products must not have adverse effects on separations chemistry. With respect to monoamides, a variety of amines and organic acid products, corresponding to the rupture of the monoamide carbonyl C–N bond, have been identified.[6,9,10] For example, Musikas reported *bis*-2-ethylhexylamine (b2EHA) and hexanoic acid as the major degradation products from the radiolysis of DEHBA.[9] In addition to b2EHA, *N*-(2-ethylhexyl)isobutyramide (MEH*i*BA), corresponding to rupture of the acyl C–N bond, was also identified for the degradation of DEH*i*BA.[6] It has been shown that the nature of the alkyl group (linear versus branched) influences ligand stability towards gamma radiolysis.[11] Drader *et al.* identified the main degradation products formed from the radiolysis of three different monamides with linear or branched chains as a function of radiation quality (alpha irradiation from the self-radiolysis of plutonium and gamma rays from an external source).[12] They found that neither radiation quality nor alkyl chain modification significantly affected the formation of ligand radiolysis products.

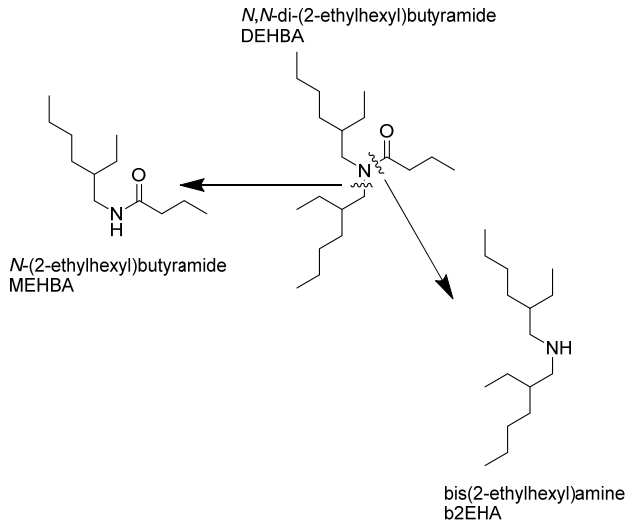


**Fig. 1** Structures of *N*,*N*-di-(2-ethylhexyl)butyramide (DEHBA) and its major degradation products: *bis*-(2-ethylhexyl)amine (b2EHA, mw = 241) and *N*-(2-ethylhexyl)butyramide, (MEHBA, mw = 199).

The most abundant monoamide degradation products arise from cleavage of the two types of C–N bonds.[1,6] The anticipated major degradation products for DEHBA are shown in Fig. 1. However, they are more than likely accompanied by lower-yield products as observed for DEH*i*BA, many of which probably are undetected and thus unreported.

Several studies have also investigated the effects of monoamide irradiation on the efficiency of actinide extraction and stripping. Studies on the extraction behaviour of gamma irradiated *N*,*N*-dialkylamides have shown that the extraction profiles for uranium and plutonium change in different ways as a function of absorbed dose and the structure of the monoamide.[3-5,11,13] Parikh *et al.* found little interference when separating uranium and plutonium using 1.1 M *di*-hexyloctanamide (DHOA) irradiated to 600 kGy.[14] Similar results were obtained by Pathak *et al.*, who also reported negligible inhibition for stripping uranium from formally 0.5 M DEH*i*BA *n*-dodecane solutions irradiated to 360 kGy while in contact with 3 – 4 M $HNO_3$.[15] Further, Drader *et al.* reported improved uranium stripping for DEH*i*BA irradiated to doses as high as 1000 kGy.[6]

As DEHBA is one of the major monoamides proposed for co-extraction of uranium and plutonium from SNF, its radiation chemistry needs to be fully quantified. In this study, the effects of gamma irradiation on DEHBA integrity and solvent system performance were investigated. DEHBA degradation rates, reaction kinetics, irradiation effects on uranium and plutonium extraction and stripping, and degradation product identification are reported for solvent system formulations representative of envisioned large-scale process conditions.

## Experimental

### Materials

Uranium-233 and plutonium-239 nitrates were sourced from on-hand stock at the Idaho National Laboratory's (INL) Radiochemistry Laboratory (RCL). DEHBA (99%) and MEHBA (99%) were supplied by Technocomm Ltd. (Wellbrae, Scotland, UK), nitric acid ($HNO_3$, *≥99.999% trace metals basis*), *n*-dodecane (*≥99% anhydrous*), dichloromethane (DCM, ≥99.8%), and b2EHA (99%) were obtained from Sigma Aldrich. Unless otherwise specified, all solvents for analyses were Fisher (Hampton, NH, USA) Optima LC/MS grade. All chemicals were used without further purification. Ultra-pure water (18.2 MΩ) was used for all aqueous solutions.

### Irradiations

*Time-Resolved Pulsed Irradiation.* Reaction kinetics of DEHBA, MEHBA, and b2EHA with the *n*-dodecane radical cation ($R^{\bullet+}$) were investigated using the picosecond pulsed electron radiolysis/transient absorption system at the Brookhaven National Laboratory (BNL) Laser Electron Accelerator Facility (LEAF).[16] Samples, comprising of varying concentrations (0 – 10 mM) of solute in 0.5 M DCM *n*-dodecane solution, were irradiated in 1.00 cm optical pathlength Suprasil cuvettes sealed with Teflon stoppers. The decay kinetics of $R^{\bullet+}$ were followed at 800 nm over 200 ns using a FND-100 silicon diode detector, and digitized by a LeCroy WaveRunner 640Zi oscilloscope (4 GHz, 8 bit). Interference filters (~10 nm bandpass) were used for wavelength selection of the analysing light. Second-order reaction kinetics were extracted by taking pseudo-first-order double-exponential fits to the decay traces and plotting as a function of solute concentration.

*Steady-State Irradiation.* Gamma irradiations of DEHBA, MEHBA, and b2EHA were performed using a Nordion Gammacell 220 Cobalt-60 irradiator unit at INL and a Shepherd 109-68 cobalt-60 irradiator unit at the Notre Dame Radiation Laboratory (NDRL). Samples consisted of either neat *n*-dodecane solutions or biphasic solvent systems contacted with an equivalent volume of aqueous 0.1 or 3.0 M $HNO_3$. Samples were irradiated in 20 mL screw-cap scintillation vials to doses up to 700 kGy, under 'deaerated' conditions – with the static, sealed vials considered deaerated upon exposure to relatively low absorbed gamma doses, owing to radiolytic-induced consumption of oxygen. Samples were irradiated in triplicate, in different positions using a jig placed in the irradiatior. The dose rate was established at each position in the jig and used to calculate the total absorbed dose for each replicate. Dosimetry was performed using Fricke solution[17], corrected for the radioactive decay of cobalt-60 and *n*-dodecane electron density $((Z_{dodecane}/A_{dodecane})/(Z_{H2O}/A_{H2O}) \times (\rho_{dodecane}/\rho_{H2O}) = 0.78)$[18], affording average dose rates of 0.82 and 1.65 Gy $s^{-1}$ for the Nordion and Shepherd irradiator units, respectively. Irradiated samples were split for analysis by the collaborating laboratories at CEA-Marcoule and INL. *G*-values were calculated from slopes of linear least squares fits to data of the measured concentrations of DEHBA, MEHBA, and b2EHA versus absorbed gamma dose.

**Analysis**

*Uranium and Plutonium Distribution Ratios.* Solvent extraction experiments were conducted using 4.0 M $HNO_3$ for organic loading and 0.1 M $HNO_3$ for organic stripping. Since DEHBA is a solvating extractant known to extract acid, the organic phases were pre-equilibrated twice with 4.0 M $HNO_3$ for 10 min at a 2:1 aqueous to organic volume ratio to ensure acid extraction equilibrium before introduction of the actinide ions. Extraction experiments were performed by contacting equal volumes (1.0 mL) of the pre-equilibrated organic phase with fresh 4.0 M $HNO_3$ solution containing radiotracer amounts of uranium-233 or plutonium-239 for 1 minute and then centrifuged for 3 minutes. The phases were then separated into individual vials and 300 µL of each phase was sampled and introduced to 10 mL of scintillation cocktail (Optima Gold). Organic stripping was then performed by contacting equal volumes (0.5 mL) of the loaded organic phase with fresh 0.1 M $HNO_3$ solution for 1 minute, centrifuged for 3 minutes, and then separated into individual vials for sampling. 300 µL samples of each phase were then introduced to 10 mL of scintillation cocktail. Both sets of samples were subsequently analysed by scintillation counting, using a PerkinElmer Tri-Carb 3180TR/SL Low Activity LSC, to determine the ratio of radioisotope activity in each phase, allowing for calculation of uranium and plutonium distribution ratios ($D_{\mathrm{M}} = \frac{[\mathrm{M}]_{\mathrm{org}}}{[\mathrm{M}]_{\mathrm{aq}}}$).

*Quantification by GC-FID. G*as chromatography with flame ionization detection (GC-FID) was used to determine the concentrations of DEHBA, MEHBA, and b2EHA, using several Agilent 7890 gas chromatographs, each equipped with an Agilent 7693 autosampler and a flame ionization detector (FID). For experiments related to the radiolysis of DEHBA, each sample was diluted by a factor of 100 in 2-propanol three different times, while for those related to the radiolysis of MEHBA and b2EHA each sample was diluted four times in 2-propanol. A separate instrument was used for each dilution replicate (three total GC instruments for the DEHBA radiolysis experiments, and four total instruments for the MEHBA and b2EHA radiolysis experiments). Prior characterization of each GC instrument has not revealed any systematic differences between them.

Each dilution replicate was injected four times, using the following conditions: a Restek Rtx-5 (30 m × 0.32 mm ID × 0.25 µm df) column with an injector temperature of 300 °C; an oven temperature of 100 °C for 1 minute, ramped to 275 °C at 15 °C $min^{-1}$ and held at 275 °C for 1 minute. The split ratio was 20:1 with 1.9 mL $min^{-1}$ flow through column. The FID temperature was 300 °C. The dilution replicate injection order was randomized to help differentiate systematic instrument drift from real trends in the samples, but the quadruple injections per dilution replicate were conducted sequentially, to reduce perturbations due to diluent evaporation.

Quantification was performed using a calibration curve with standards prepared from neat DEHBA, MEHBA, and b2EHA dissolved in 2-propanol. Six calibration points and a blank were used to construct calibration curves for each compound on each instrument. Each standard was injected four times and analysed in order of increasing concentration. Quality control (QC) standards made at three different concentrations were analysed at the mid-point of the analysis and at the end to ensure validity of the calibration curve through-out the entire measurement period. End-run QC standards were placed in separate vials from the mid-run QC standards to reduce the effects of diluent evaporation.

*Quantification of MEHBA and b2EHA with GC-MSMS.* Coelution of MEHBA and b2EHA from irradiated DEHBA samples, required quantification by gas chromatography with tandem mass spectrometry detection (GC-MSMS). Quantification was performed using a Shimadzu Scientific GCMS-TQ8040 gas chromatography with a triple-quadrupole mass spectrometer using electron impact ionization and multiple reaction monitoring (MRM). Samples were diluted by a factor of 100 in 2-propanol. All three dilution replicates were run on the same instrument. The conditions for the mass spectrometer were: 280 °C interface temperature; 260 °C ion source temperature; and 70 eV electron energy. All gas chromatograph conditions and quantification procedures were the same as described for quantification by GC-FID (see above).

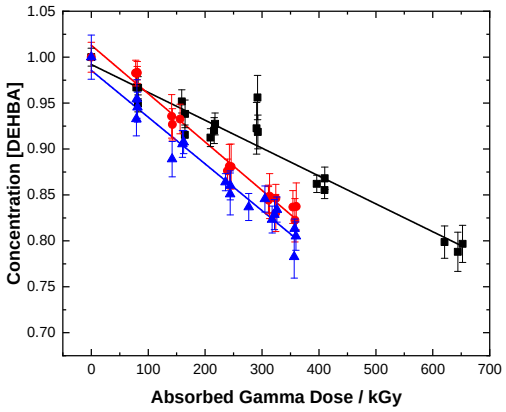


**Fig. 2** Normalized concentration of DEHBA as a function of absorbed dose from gamma irradiation (0.82 Gy $s^{-1}$) of 1.0 M DEHBA *n*-dodecane solution: organic-only (■), and biphasic contacted with 0.1 (●) and 3.0 (▲) M $HNO_3$. Error bars are 99% confidence intervals calculated from four measurement replicates. Solid lines are weighted linear fits to data.

*Degradation Product Identification using ESI-MS.* The mass spectrometry measurements were recorded in positive ionization mode using a Bruker Daltonics micrOTOF-Q II quadrupole time-of-flight mass spectrometer equipped with an electrospray interface. A syringe infusion pump, Cole Palmer, delivered the sample at a rate of 90 µL $h^{-1}$ to the electrospray source. The QTOF was mass calibrated daily using an Agilent (G2421A) ES-TOF tuning solution. The capillary voltage was set to -4500 V with an end-plate offset voltage of −500 V. Nitrogen was employed as the drying and nebulizing gas. The drying gas flow rate was set to 4.0 L $min^{-1}$, the nebulizing gas pressure was set to 0.4 bar, and the source temperature was set to 180 °C. Spectra were acquired over a mass range of m/z 40–3000. Tandem mass spectra were obtained from collision-induced dissociation (CID) with nitrogen.

Samples were diluted by a factor of 10000 in 1:1 acetonitrile/water prior to injection into the ESI-MS. To favour ionization of compounds and avoid the formation of sodiated adducts, samples irradiated in contact with 0.1 M $HNO_3$ were acidified before analysis by the addition of 1 drop of 1.0 M $HNO_3$. The ESI-MS measurements were taken within a short time after sample preparation to avoid any solvent influences on the speciation of degradation products. Species were identified by comparison with an isotopic pattern calculated using the software DataAnalysis 4.0. CID experiments were used to help identify the structures of various species through fragmentation studies.

*Degradation Product Identification using LC-ESI-MS.* Liquid chromatography coupled to a mass spectrometer with an electrospray ionization source (LC-ESI-MS) can be significantly more sensitive for some compounds than GC-MS. Additionally, the mass spectrometer used here, a quadrupole time-of-flight, has a mass accuracy of better than 2 millimass units, enabling unambiguous molecular formula for compounds in the mass range of potential DEHBA degradation products. Irradiated samples of DEHBA were analysed using a Dionex Ultimate 3000 ultra-high-pressure liquid chromatograph (UHPLC) with a Bruker micrOTOF-Q II quadrupole time-of-flight mass spectrometer with electrospray ionization. Separation was achieved using a Phenomenex Kinetex® 1.7 µm XB-C18 column (150 × 2.1 mm) with a flow rate of 400 µL $min^{-1}$. The aqueous mobile phase component was water with 0.1% (v/v) formic acid, and the organic component was acetonitrile with 0.1% (v/v) formic acid. A gradient elution profile was used. The column was equilibrated at 30% organic for 5 minutes, followed by a ramp to 95% organic over 4 minutes. The mobile phase was held at 95% organic for 6 minutes, followed by a return to 30% organic in 0.5 minutes.

The mass spectrometer source and tuning parameters can be found in the Supplementary Information (SI). Mass calibration was achieved using sodium formate clusters by infusing a tune mixture during each chromatographic run via a divert valve on the mass spectrometer. Using this mass calibration procedure, the mass spectrometer routinely achieves mass accuracy of ≤ 2 millimass units (mDa).

*FT-IR analysis.* Organic phase samples were analysed with a Bruker Vertex 70 spectrometer equipped with an attenuated total reflectance cell. All spectra were collected between 400–4000 $cm^{-1}$, using 32 scans and a resolution of 4 $cm^{-1}$.

## Results and Discussion

### Degradation Rate

DEHBA dissolved in *n*-dodecane was irradiated as organic-only, and biphasic in contact with a 0.1 or 3.0 M $HNO_3$ aqueous phase. The normalized concentration of DEHBA as a function of absorbed gamma dose for each of the three conditions is shown in **Fig. 2** (measured concentration data without normalization are given in *SI*), and the corresponding *G*-values given in Table 1.

**Table 1.** Radiolytic yields for independent gamma irradiation of DEHBA, MEHBA, and b2EHA *n*-dodecane solutions obtained from linear fits to measured concentration changes with absorbed dose for various solution conditions.

| **Solution Conditions** | **G-Value** (μmol $J^{-1}$) | | |
|---|---|---|---|
| | **DEHBA** | **MEHBA** | **b2EHA** |
| Organic-Only | -0.31 ± 0.02 | -0.08 ± 0.01 | -0.12 ± 0.01 |
| 0.1 M $HNO_3$ Contact | -0.53 ± 0.02 | -0.12 ± 0.01 | *hydrolysis* |
| 3.0 M $HNO_3$ Contact | -0.49 ± 0.02 | *hydrolysis* | *hydrolysis* |

DEHBA degrades linearly with absorbed gamma dose under all three conditions. The rate of DEHBA degradation for organic-only conditions ($G$ = -0.31 ± 0.02 μmol $J^{-1}$) is lower than when irradiated in contact with an aqueous phase, indicating significant interplay between organic and aqueous radiolysis products.

Under organic-only conditions, the *n*-dodecane radical cation ($R^{\bullet+}$) is thought to be the major reactive species inducing ligand degradation:

$$\text{Solute} + R^{\bullet+} \rightarrow [\text{Solute}]^{\bullet+} + R, \qquad (1)$$

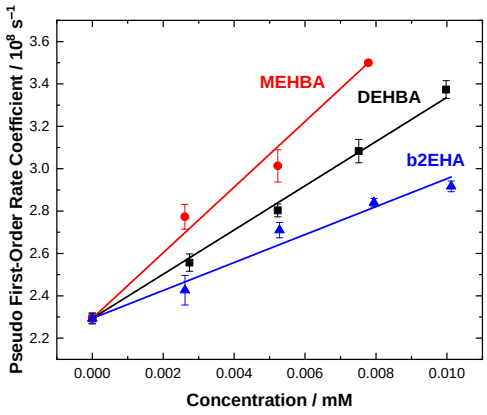


**Fig. 3.** Concentration dependence of pseudo-first-order rate coefficients for the reaction of the *n*-dodecane radical cation with DEHBA (■), MEHBA (●), and b2EHA (▲). Solid lines are weighted linear fits, with slopes corresponding to the second-order rate coefficient: $k_{DEHBA}$ = (1.08 ± 0.03) × $10^{10}$ $M^{-1}$ $s^{-1}$, $k_{MEHBA}$ = (1.49 ± 0.08) × $10^{10}$ $M^{-1}$ $s^{-1}$; and $k_{b2EHA}$ = (6.52 ± 0.40) × $10^{9}$ $M^{-1}$ $s^{-1}$.

for which a rate coefficient ($k$) of (1.52 ± 0.11) × $10^{10}$ $M^{-1}$ $s^{-1}$ has been reported for DEH*i*BA.[6,19] The corresponding reaction kinetics for $R^{\bullet+}$ with DEHBA was determined in this study using time-resolved picosecond pulsed radiolysis techniques, for which the associated kinetic data are given in Fig. 3 (see *Reaction Kinetics* in SI). For DEHBA, a second-order rate coefficient of $k$ = (1.08 ± 0.03) × $10^{10}$ $M^{-1}$ $s^{-1}$ was calculated, which is approximately 41% slower than that for DEH*i*BA, but nevertheless considered diffusion limited and indicative of a critical degradation pathway. The lifetime of $R^{\bullet+}$ in *n*-dodecane has been reported as 2 ns,[20] owing to rapid recombination with geminate and non-geminate electrons. Therefore, any perturbation in the composition of the organic phase that lends itself to either adding additional reactive species to the suite of available radiolysis products or extending the lifetime of $R^{\bullet+}$ through electron scavenging has the potential to enhance the rate of DEHBA degradation. In the presence of an aqueous phase, mass transfer and complexation allow for a fraction of aqueous medium to be drawn into the organic phase, thereby adding water and $HNO_3$ to its composition. The energy deposited by ionizing radiation will be partitioned between the constituents of the medium proportional to their contribution to the total electron density of the medium.[21] Consequently, direct radiolysis will be induced in both extracted water and $HNO_3$, the extent of which will reflect their respective electron fractions relative to DEHBA and *n*-dodecane.

For 0.1 M $HNO_3$ contacts, the potential organic phase electron fraction contribution of extracted $HNO_3$ is negligible and thus any additional DEHBA degradation would be attributed to the products of extracted water radiolysis:

$$H_2O \rightsquigarrow e^-, H^{\bullet}, {}^{\bullet}OH, H_2O_2, H_2, H_{aq}^{+}, \qquad (2)$$

which clearly enhances the rate of DEHBA degradation ($G$ = -0.53 ± 0.02 μmol $J^{-1}$). Increasing the concentration of $HNO_3$ to 3.0 M increases the electron fraction of extracted $NO_3^-$/$HNO_3$, and similarly accelerates the rate of DEHBA degradation ($G$ = -0.49 ± 0.02 μmol $J^{-1}$), relative to organic-only solution. These observations are attributed to: (i) radiolytic formation of additional powerful oxidizing species, such as hydroxyl ($^{\bullet}OH$, $E^o$ = 2.7 V in water)[22] and nitrate ($^{\bullet}NO_3$, $E^o$ = 2.3 – 2.7 V in water)[23] radicals, that have been extensively shown to induce ligand degradation;[22,24] and (ii) scavenging of non-geminate electrons by $NO_3^-$ and $^{\bullet}OH$, thereby extending the lifetime and availability of $R^{\bullet+}$ and inhibiting potential regenerative processes (reaction 7):[22,25]

$$HNO_3 \rightsquigarrow e^-, {}^{\bullet}NO_3, HNO_2, O \quad (3)$$

$$NO_3^- + e_{pre}^- \rightarrow NO_3^{\bullet 2-} \quad k_{H2O} = 1 \times 10^{13}\ M^{-1}\ s^{-1} \quad (4)$$

$$NO_3^- + e_{aq}^- \rightarrow NO_3^{\bullet 2-} \quad k_{H2O} = 9.7 \times 10^{9}\ M^{-1}\ s^{-1} \quad (5)$$

$$^{\bullet}OH + e_{aq}^- \rightarrow OH^- \quad k_{H2O} = 3.0 \times 10^{10}\ M^{-1}\ s^{-1} \quad (6)$$

$$[DEHBA]^{\bullet+} + e^- \rightarrow DEHBA. \quad (7)$$

With regards to the presence of $^{\bullet}OH$ and $^{\bullet}NO_3$, reactions via hydrogen atom abstraction (reaction 8) would produce carbon-centered radicals ($R^{\bullet}$), and under initial aerated conditions, oxygen would add to these to further enhance degradation rates, possibly via decay of the resulting tetroxides (R–O–O–O–O–R):[26]

$$R + {}^{\bullet}OH/{}^{\bullet}NO_3 \rightarrow R^{\bullet} + H_2O/HNO_3 \quad (8)$$

$$R^{\bullet} + O_2 \rightarrow RO_2^{\bullet} \quad (9)$$

$$RO_2^{\bullet} + RO_2^{\bullet} \rightarrow R–O–O–O–O–R \quad (10)$$

$$R–O–O–O–O–R \rightarrow Products. \quad (11)$$

However, loss of dissolved oxygen will occur at relatively low absorbed doses, which then switches peroxyl radical chemistry to carbon-centered radical combination reactions:

$$R_1^{\bullet} + R_2^{\bullet} \rightarrow Products. \quad (12)$$

The subtle difference in contacted $G$-values is likely due to the greater reactivity of $^{\bullet}OH$ versus $^{\bullet}NO_3$, as $^{\bullet}OH$ rate coefficients are typically faster in water.[22,24] Unfortunately, rate coefficients for these processes have not been determined in the organic phase.

Overall, contact with an oxidizing environment enhances the rate of DEHBA degradation in *n*-dodecane. These findings on the effect of chemical environment (i.e., contacted solution composition) are in contrast to previous DEH*i*BA work.[6] The differences in DEH*i*BA degradation rates with irradiation conditions may have been concealed by the higher analytical uncertainties reported previously. Here, lower uncertainties were obtained by a combination of GC-FID method development and a rigorous analytical protocol. Regardless of the proposed mechanisms, the radiolytic degradation rate of DEHBA in contact with an aqueous phase is comparable to the average $G$-value reported for DEH*i*BA[6] – and somewhat faster than that reported for TBP (-0.37 μmol $J^{-1}$)[7]. This rate is comparable to those reported for many monoamides,[3-4] although the methylbutylalkylmonoamides appear to degrade somewhat faster.[5]

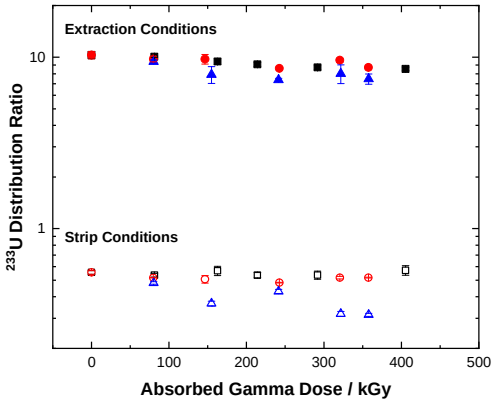


**Fig. 4** Uranium distribution ratios under extraction and strip conditions as a function of absorbed gamma dose for pre-irradiated DEHBA *n*-dodecane solution: organic-only (■), and biphasic contacted with 0.1 (●) or 3.0 (▲) M $HNO_3$.

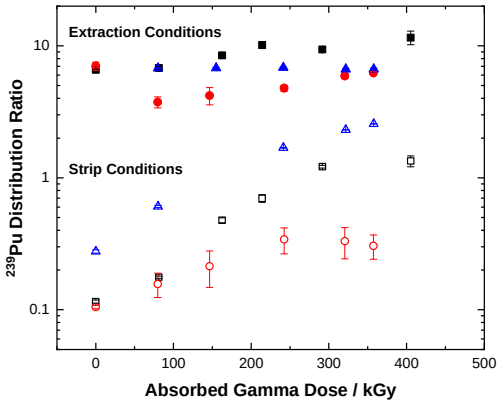


**Fig. 5** Plutonium distribution ratios under extraction and strip conditions as a function of absorbed gamma dose for pre-irradiated DEHBA *n*-dodecane solution: organic-only (■), and biphasic contacted with 0.1 (●) or 3.0 (▲) M $HNO_3$.

**Effects on Uranium and Plutonium Partitioning and Stripping**

The impact of gamma irradiation on DEHBA solvent extraction performance was determined by performing batch contacts of the irradiated organic phase with 4.0 M $HNO_3$ spiked with uranium and plutonium, followed by a 0.1 M $HNO_3$ strip. Distribution ratios

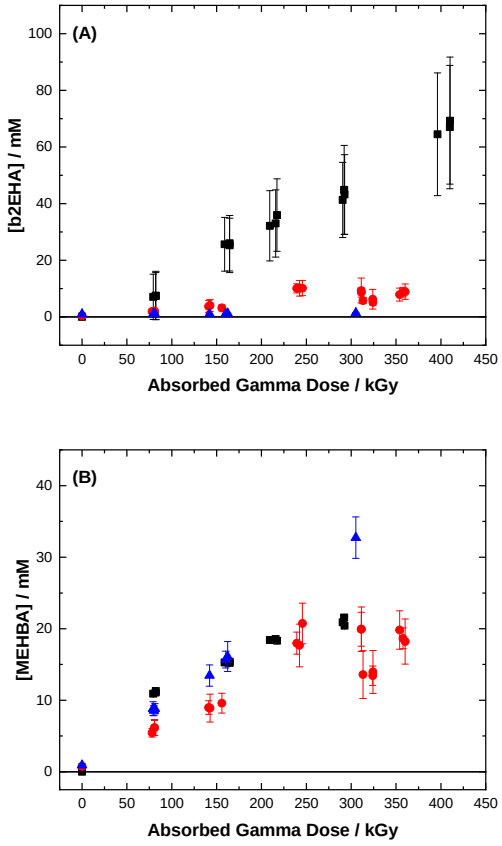


**Fig. 6** Ingrowth of b2EHA (**A**) and MEHBA (**B**) from the gamma irradiation (0.82 Gy $s^{-1}$) of 1.0 M DEHBA *n*-dodecane solution: organic-only (■), and biphasic contacted with 0.1 (●) and 3.0 (▲) M $HNO_3$. Error bars are 99% confidence intervals calculated from four measurement replicates.

($D$) for uranium and plutonium under extraction (4.0 M $HNO_3$) and strip (0.1 M $HNO_3$) process conditions are given in Fig. 4 and 5, respectively, under all investigated solvent system permutations.

For uranium extraction, Fig. 4, $D_U$ may have decreased slightly with absorbed gamma dose for all investigated conditions, however the decrease is within experimental error. Drader *et al.* reported a constant $D_U$ for all investigated DEH*i*BA permutations out to the higher absorbed dose of 1000 kGy.[6] The possible loss of extraction $D_U$ for DEHBA here is not particularly concerning, as the $D_U$ decreased from about 10 to 8.5 in going from 0 to 400 kGy, corresponding to 91% and 89% uranium extracted, respectively. Further, the absorbed gamma doses used in these experiments are high compared to the envisioned lifetime exposure of a given solvent. For the corresponding uranium strips in Fig. 4, $D_U$ remained almost constant except for a decrease for samples irradiated in contact with the highest acidity, suggesting interference by acid hydrolysis products. These observations suggest progressively easier recovery of uranium for samples irradiated in the presence of acid, which is advantageous for solvent extraction performance. From the standpoint of process application, there is little difference in the uranium extraction performance of the monoamides DEHBA and DEH*i*BA.

With regards to plutonium extraction, Fig. 5, $D_{Pu}$ is very much dependent on the chemical environment during irradiation. Under organic-only irradiation conditions, $D_{Pu}$ showed a steady increase not observed for uranium. This behaviour is indicative of a degradation product being formed that is a more effective complexing agent for plutonium than DEHBA. Furthermore, this product's formation is either inhibited when irradiated in contact with an aqueous phase (e.g., by acid hydrolysis or $HNO_3$ radiation chemistry), or it is water miscible, partitioning into the aqueous phase, since $D_{Pu}$ for the corresponding acid contacts do not show the same increase in extraction with absorbed dose. Ruiker *et al.* also reported increasing $D_{Pu}$ with absorbed dose, for three investigated alkyl ethyhexylamides, although their data differed in showing an initial induction period at low doses.[3] Their samples were irradiated in *n*-dodecane that had been pre-equilibrated with 3.5 M $HNO_3$.

The corresponding plutonium strips shown in Fig. 5, are similarly complex. For organic-only irradiation conditions, $D_{Pu}$ steadily increases with absorbed dose. Plutonium retention is likely by the same species responsible for enhanced extraction under organic-

only conditions. Interestingly, 3.0 M $HNO_3$ contacts during irradiation promote the formation of a second distinct interfering species that exhibits particularly strong plutonium retention but plays a minimal role in plutonium extraction. Although retention of plutonium in the organic phase during stripping may be undesirable for plutonium recovery, a selective uranium strip can be envisioned based on these results. Further, in the presence of higher metal loading conditions that might occur in a solvent extraction process, the effects of small amounts of degradation products may be less dramatic than shown here in tracer studies.

**DEHBA Degradation Products**

Based on previous monoamide studies, the expected products from DEHBA radiolysis were b2EHA (Fig. 1, $[M+H^+]$ $m/z$ = 242) and butanoic acid, both resulting from cleavage of the acyl C–N bond. In addition, we expected to see MEHBA (Fig. 1, $[M+H^+]$ $m/z$ = 200) and 2-ethylhexane from rupture of the alkyl C–N bond, based on previous analogous work with DEH*i*BA.[6] Both b2EHA and MEHBA were identified, but the corresponding carboxylic acid and aliphatic products were not detected (see *Degradation Product Analysis* in *SI*. This is expected, because the mass of the carboxylic acid is below the low-mass cut-off of the mass spectrometer, and the aliphatic compound does not produce an ion with electrospray.

The radiolytic ingrowth of b2EHA and MEHBA from the gamma radiolysis of 1.0 M DEHBA are given in Fig. 6. For organic-only irradiation conditions, the amount of b2EHA increases linearly, while the rate of formation of MEHBA slows with absorbed dose due to secondary radiolytic processes, i.e., the concentration of MEHBA is sufficiently high to compete with DEHBA for radiolysis products. This interpretation is supported by corresponding rate coefficients measured for the reaction of $R^{\bullet+}$ with b2EHA ($k$ = (6.60 ± 0.25) × $10^9$ $M^{-1}$ $s^{-1}$) and MEHBA ($k$ = (1.55 ± 0.01) × $10^{10}$ $M^{-1}$ $s^{-1}$) – the lower $R^{\bullet+}$ rate coefficient for b2EHA means higher concentrations of b2EHA are necessary to compete for $R^{\bullet+}$, relative to MEHBA and DEHBA. The complementary gamma irradiation experiment results given in Fig. 7 confirm that both products are themselves susceptible to radiolytic degradation. Fig. 7 shows that both b2EHA and MEHBA degrade linearly with absorbed dose under organic-only conditions – complimentary acid contacts were not possible due to hydrolysis of b2EHA and MEHBA. Interestingly, b2EHA degrades faster than MEHBA, which is counter intuitive when considering their respective $R^{\bullet+}$ rate coefficients. This indicates additional chemistries are occurring, e.g., reaction of b2EHA with other primary and/or secondary *n*-dodecane radiolysis products, such as ubiquitous solvated electrons or carbon-centered radicals.

As shown in Fig. 6, the yield of b2EHA, but not MEHBA, versus absorbed dose is dependent on solution conditions during irradiation. The presence of an aqueous phase during irradiation suppresses b2EHA formation or facilitates partitioning into the aqueous phase, which corresponds to the much less dramatic effects on plutonium extraction and retention distribution ratios seen in Figure 5. Thus, the increased extraction efficiency and retention of plutonium for samples irradiated under organic-only conditions are attributed to b2EHA formation and its subsequent complexation of plutonium. In contrast, Drader *et al.* reported that the monoamide product MEHBA, but not the amine product b2EHA, formed a Pu complex, as detected by mass spectrometric experiments. A mixed species containing the original ligand and its amidic degradation product was reported to be $Pu(DEHBA)(MEHBA)(NO_3)^{3+}$ in that work.[12] Complexes containing b2EHA were not reported. However, when we contacted a solution of MEHBA/*n*-dodecane with 4.0 M $HNO_3$ spiked with plutonium, we measured negligible extraction, which casts doubts on MEHBA being responsible for the progressive increase in $D_{Pu}$ with absorbed dose reported here in the condensed phase. Further, MEHBA exhibits negligible dependence on the concentration of entrained $HNO_3$ during irradiation as shown in Fig. 6 (**B**).

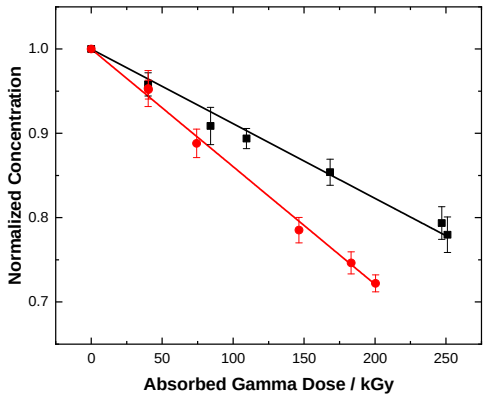


**Fig. 7** Normalized concentrations of MEHBA (■) and b2EHA (●) *n*-dodecane solutions as a function of absorbed dose from gamma irradiation (1.65 Gy $s^{-1}$) of organic-only conditions. Solid lines are weighted linear fits to data.

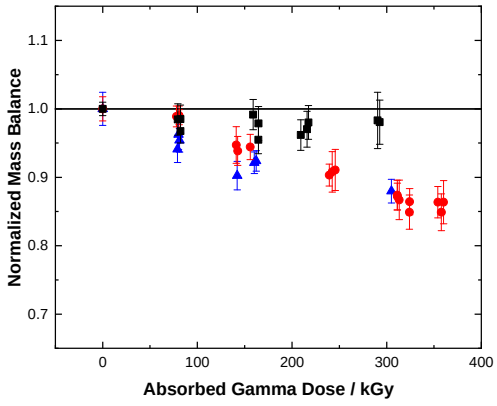


**Fig. 8** Normalized mass balance, assuming radiolysis of a single DEHBA molecule yields either one MEHBA or one b2EHA molecule, from the gamma irradiation (0.82 Gy $s^{-1}$) of 1.0 M DEHBA *n*-dodecane solution: organic-only (■) and biphasic contacted with 0.1 (●) and 3.0 (▲) M $HNO_3$.

Assuming the two fragmentation pathways proposed in Fig. 1 are dominant, radiolytic fragmentation of a single DEHBA molecule should yield either one MEHBA or one b2EHA molecule. Therefore, the sum of these three species (DEHBA, MEHBA, and b2EHA), should remain constant, affording mass closure for the degradation process. This is demonstrated in Fig. 8 for organic-only conditions, where, within experimental uncertainty, the total concentration remains at ~1.0 M throughout, supporting our hypothesis. Comparison of the amounts of MEHBA and b2EHA gives an indication of the percentage of DEHBA molecules that fragment according to each proposed pathway. Except for the earliest doses, where the total concentration of each degradation product is very small, these data suggest that when irradiated under organic-only conditions, approximately 60% of the radiolytically degraded DEHBA molecules fragment to produce b2EHA and its butanoic acid partner, while the remaining 40% fragment to produce MEHBA and its 2-ethylhexane partner. This distribution ratio was unexpected, as there are twice as many alkyl C–N bonds to break. Further, bond dissociation energy (BDE) calculations[12] for monoamide surrogates of DEHBA indicate that the alkyl C–N bond is weaker than the acyl C–N bond, also suggesting that the fragmentation pattern, based on thermodynamics, should be the reverse. However, the difference in BDEs between these two bonds is relatively low (~12 kJ $mol^{-1}$), and radiolytic processes are typically kinetically driven, favouring attack at the less sterically hindered acyl C–N bond.

Mass balance is not achieved for samples irradiated in the presence of an aqueous phase (Fig. 8). As was mentioned above, the steady-state concentration of b2EHA significantly decreases when the organic phase is contacted with increasing concentrations of aqueous $HNO_3$, Fig. 6 (**A**). This dependence likely reflects a combination of acid hydrolysis, partitioning into the aqueous phase, and/or additional reactions with radiolysis products originating from extracted water and/or $HNO_3$. The ingrowth of MEHBA on the other hand, appears to be more stable with respect to changes in chemical environment, exhibiting less of a dependence on $HNO_3$ concentration, as seen in Fig. 6 (**B**). In order to gain information about the minor degradation products formed under different experimental conditions, ESI-MS spectra were collected for each organic solution. Examples of these spectra are reported in *SI* along with CID spectra of the main ions. Further, Table S1 includes the degradation products observed under different experimental conditions. The species are identified thanks to their isotopic pattern and their fragmentation spectra. In addition to the presence of DEHBA, MEHBA and b2EHA, several species at *m/z* = 326.0, 310.2, and 256.2 are quite significant. The species at *m/z* = 326.0 and 310.2 are identified as DEHBA with a ketone function in its skeleton, and DEHBA with a double bond in the structure, respectively. Compounds at *m/z* = 326.0 and 256.2 correspond to oxidation of a $CH_2$ group into a C=O group on the alkyl chain of DEHBA and b2EHA, respectively. These may be formed via hydrogen abstraction, followed by reaction with $^{\bullet}OH$, and oxidation of the resulting alcohol to the corresponding ketone functionality. The compound at *m/z* = 310.2 was observed for all experimental conditions and corresponds to the abstraction of two hydrogen atoms (or disproportionation) from DEHBA to form a double bond. All of these compounds were previously reported for the gamma irradiation of DEH*i*BA in the presence of $HNO_3$, and alpha irradiation of DEHBA in presence of plutonium nitrate.[6,12] In the presence of 0.1 M $HNO_3$, several heavier species (*m/z* = 551.7, 533.5, 480.5, and 410. 5) were observed, further highlighting the importance of chemical environment on dictating the radiolytic pathways available to DEHBA. These new species were also reported for DEH*i*BA in the absence of an aqueous phase and identified as recombination products:[6] *m/z* = 551.7 is an addition product of the monoamide with the amine di-ethylhexylamine (DEHA); *m/z* = 480.5 (monoamide + *n*-dodecane) and 410.5 (DEHA + *n*-dodecane). The peak at *m/z* = 533.5 was unidentified. For samples irradiated in the presence of concentrated $HNO_3$, these species were completely absent.

IR analyses, shown in Fig. 9, indicate that species containing carboxyl groups were produced. Irradiation in the presence of 0.1 M $HNO_3$ (Fig. 9 (**A**)) showed modification to the 1000-1100 $cm^{-1}$ area of DEHBA's IR spectra, indicating the presence of a C–O stretch. Changes to the spectra for 3.0 M $HNO_3$ contacted samples (Fig. 9 (**A**)) were more dramatic and show new vibration bands. For example, prior to irradiation, there is a $HNO_3$-monoamide vibration band at 1590 $cm^{-1}$ assigned to a C=O group bonded to $HNO_3$, and bands at 1284, 943, 685, and 636 $cm^{-1}$, which are consistent with the presence of undissociated $HNO_3$ in the organic phase.[27,28] In contrast, after irradiation, peaks appear between 1732-1715 $cm^{-1}$ and a shoulder at 1630 $cm^{-1}$, complemented by a

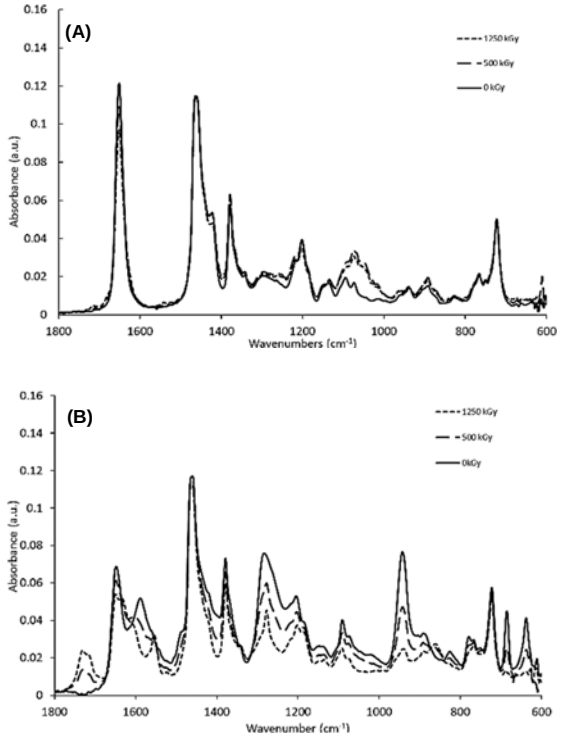


**Fig. 9** IR spectra of formally 1.0 M DEHBA in *n*-dodecane: **(A)** contacted with 0.1 M $HNO_3$ before and after gamma irradiation; and **(B)** pre-contacted with 3.0 M $HNO_3$, and post-contacted with 4.0 M $HNO_3$ after gamma irradiation.

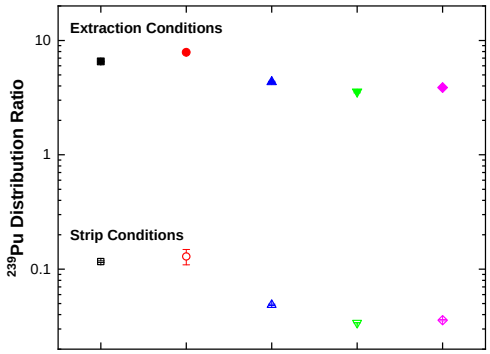


**Fig. 10** Plutonium distribution ratios under extraction and strip conditions for non-irradiated *n*-dodecane solutions of: 1.0 M DEHBA (■/□); 80 mM b2EHA + 0.8 M DEHBA (●/○); 80 mM butanoic acid + 0.8 M DEHBA (▲/△); 20 mM MEHBA + 0.8 M DEHBA (▼/▽); and 20 mM ethylhexene + 0.8 M DEHBA (◆/◇).

decrease in vibration bands associated with the C=O–$HNO_3$ stretch (i.e., 1590, 1284, 943, 885, 682, and 633 $cm^{-1}$). This is consistent with the radiolysis of extracted $HNO_3$. Appearance of the peak at 1730 $cm^{-1}$ may indicate formation of either a new carboxylic acid,[3,4,9,10,29-31] possibly attributed to butanoic acid, or formation a ketone functionality, while development of the shoulder peak (1630 $cm^{-1}$) suggests formation of a new amide species, possibly MEHBA. Organic acids with significant organic phase solubility have been implicated in decreased stripping efficiency for other solvent systems.[32,33] An organic acid formed under acid contacted conditions during irradiation, which would enhance oxidative degradation of DEHBA, would explain both the changes in IR spectra and the rapidly increasing strip $D_{Pu}$ for samples irradiated in the presence of 3.0 M $HNO_3$. Given the loss of b2EHA under oxidizing conditions, such an organic soluble acid may be derived from this amine. It is clear that the presence of acid during irradiation alters the degradation mechanisms responsible for DEHBA radiolysis. These results are similar to those previously reported for

DEH*i*BA when irradiated in the presence and absence of an acidic aqueous phase.[6] Thus, two competitive degradation schemes can be envisaged for the two $HNO_3$ concentration regimes investigated here, these are given in *SI Fig. S11* and *S12*.

To further investigate the role of DEHBA's degradation products in plutonium extraction, non-irradiated organic phases were prepared containing selected decomposition products. To simulate the effect of irradiating an organic-only DEHBA *n*-dodecane solution to ~400 kGy, solutions containing DEHBA, b2EHA, and MEHBA of approximately 0.8 M, 80 mM, and 20 mM, respectively, were prepared. Stoichiometric amounts of butanoic acid and 2-ethylhexene were also used – 2-ethylhexene was chosen because cleavage of the alkyl C–N bond initially yields the 2-ethylhexane radical, which is prone to dehydrogenation and formation of the corresponding olefin. A series of plutonium partitioning experiments were performed to de-convolute the roles of these degradation products on $D_{Pu}$. The results are shown in Fig. 10. For both extraction and strip conditions, $D_{Pu}$ is significantly enhanced in the presence of b2EHA, relative to 1.0 M DEHBA *n*-dodecane solution. This provides direct evidence for plutonium complexation by b2EHA and explains the enhanced $D_{Pu}$ values in Fig. 5 for organic-only conditions. Further, Fig. 10 shows that the MEHBA, butanoic acid, and 2-ethylhexene solutions exhibit reduced $D_{Pu}$ by approximately the same extent for both extraction and strip conditions, attributed to modifications of the organic solvent. This demonstrates that MEHBA, butanoic acid, and 2-ethylhexene are poor plutonium complexants, and cannot explain the observed increased plutonium retention, but may be responsible to some extent for the decrease in $D_{Pu}$ seen for 0.1 M $HNO_3$ contacts in Fig. 5 strip conditions. These observations indicate that the remaining, unidentified, degradation product, responsible for the increase in strip $D_{Pu}$ for 3.0 M $HNO_3$ contacts only, is a subsequent hydrolytic and/or radiolytic degradation product. This species could be one of the observed bifunctional compounds (e.g., *m/z* = 326) with a high affinity for plutonium, or a mixed species including DEHBA, [Pu-DEHBA-degradation product], leading to synergistic complexation.

**Colour Development**

There is additional evidence of unidentified degradation products in irradiated DEHBA *n*-dodecane solution. It is not unusual for organic solvents to develop a yellow tint when irradiated, and the irradiation of DEHBA *n*-dodecane solutions is no exception, especially when in contact with $HNO_3$. However, the irradiated organic-only and 0.1 M $HNO_3$ contacted DEHBA *n*-dodecane solutions undergo dramatic colour changes when later contacted with fresh 4.0 M $HNO_3$ solutions during solvent extraction experiments. The colour developed is an intense rose-red colour (*Fig. S13*), which increases in intensity with absorbed gamma dose. This colour development occurs in the absence of uranium and plutonium, and thus cannot be attributed to actinide metal ion complexation; suggesting $HNO_3$ complexation or a $HNO_3$ initiated reaction. Subsequent stripping of the organic phase does not strip this intense colour. Further, this colour cannot be attributed to b2EHA, MEHBA, butanoic acid, or 2-ethylhexene, as the 4.0 M $HNO_3$ contacts performed for Fig. 10 did not give any colour change. However, when DEHBA *n*-dodecane solution is irradiated in contact with 3.0 M $HNO_3$, the rose-red colouration was not observed, even with subsequent contact of the irradiated solvent with fresh 4.0 M $HNO_3$.

The coloured species is therefore attributed to a DEHBA radiolysis product that complexes or reacts with $HNO_3$ but forms only in the absence of high concentrations of $HNO_3$. Its dramatic appearance occurred under the same solution irradiation conditions that showed increased plutonium extraction, suggesting it may be a degradation product of b2EHA and a precursor to the degradation product attributed to plutonium retention under strip conditions.

## Conclusions

The rate of DEHBA degradation by gamma radiolysis was found to be slow for organic-only conditions (-0.31 ± 0.02 μmol $J^{-1}$) and slower than that reported for TBP (-0.37 μmol $J^{-1}$).[6,7] Degradation rates in the presence of the aqueous phase were higher, an average of -0.51 ± 0.02 μmol $J^{-1}$ . Oxidizing solvent system conditions, achieved through acidic aqueous contacts, enhanced rates of DEHBA degradation by up to 65%. A gradual but minor loss in uranium extraction efficiency with absorbed gamma dose was measured under all solution irradiation conditions, although stripping efficiency was either unchanged or improved. Plutonium behaviour was more complex. An increase in extraction, $D_{Pu}$, with absorbed gamma dose was recorded for organic-only conditions, but not for acid contacts. Increasing strip $D_{Pu}$ values were found for organic-only and in the presence of highly acidic $HNO_3$ solutions, which surpassed 1.0 by 250 kGy. This suggests the possibility of a uranium-plutonium co-extraction, followed by selective stripping of these two important actinides.

Two of the major DEHBA degradation products (b2EHA and MEHBA) were identified and quantified by mass spectrometry and found to sufficiently account for mass closure up to ~300 kGy when no aqueous phase was present. Enhanced plutonium extraction and decreased stripping efficiency are attributed to b2EHA and potentially its degradation products. Numerous other oxidation products are suggested by IR analysis for solutions irradiated in contact with the aqueous phase, and the appearance of colour changes under certain conditions are the visual evidence of unidentified radiolysis products, despite a rigorous search using multiple analytical techniques. Kinetic measurements for $R^{\bullet+}$ with DEHBA, b2EHA, and MEHBA have been performed, demonstrating fast reactivity, but also the importance of other radiolytic pathways in accounting for total degradation.

## Conflicts of interest

There are no conflicts to declare.

## Acknowledgements

This research has been funded by the US Department of Energy (DOE) Assistant Secretary for Nuclear Energy, under the Material Recovery and Waste Form Development Campaign, DOE-Idaho Operations Office Contract DE-AC07-05ID14517 and DE-NE0008406 Nuclear Energy Universities Program (NEUP) grant. Organic-only MEHBA and b2EHA gamma irradiations reported herein were performed at the Notre Dame Radiation Laboratory (NDRL). The NDRL is supported by the Division of Chemical Sciences, Geosciences and Biosciences, Basic Energy Sciences, Office of Science, US-DOE through Award No. DE-FC02-04ER15533. Picosecond pulsed electron irradiations reported herein were performed using the BNL LEAF of the BNL Accelerator Center for Energy Research, supported by the US-DOE Office of Basic Energy Sciences, Division of Chemical Sciences, Geosciences, and Biosciences under contract DE-SC0012704.

The authors would like to thank the DOE-European Commission collaboration, through the Safety of Actinide Separation Processes (SACSESS) and GEN IV Integrated Oxide Fuels Recycling Strategies (GENIORS) projects, for supporting this research effort.

## Notes and references

(1) G. M. Gasparini, and G. Grossi, *Solvent Extraction and Ion Exchange*, 1986, **4 (6)**, 1233.
(2) K. McCann, J. A. Drader, and J. C. Braley, *Separation & Purification Reviews,* 2018, **47 (1)**, 49.
(3) P. B. Ruikar, M. S. Nagar, and M. S. Subramanian, *Journal of Radioanalytical and Nuclear Chemistry*, 1993, **176 (2)**, 103.
(4) P. B. Ruikar, M. S. Nagar, M. S. Subramanian, K. K. Gupta, N. Varadarajan, and R. K. Singh, *Journal of Radioanalytical and Nuclear Chemistry*, 1995, **196**, 171.
(5) P. B. Ruikar, M. S. Nagar, M. S. Subramanian, K. K. Gupta, N. Varadarajan, and R. K. Singh, *Journal of Radioanalytical and Nuclear Chemistry*, 1995, **201 (2)**, 125.
(6) J. Drader, G. Saint-Louis, J. M. Muller, M. C. Charbonnel, P. Guilbaud, L. Berthon, K. M. Roscioli-Johnson, C. A. Zarzana, C. Rae, G. S. Groenewold, B. J. Mincher, S. P. Mezyk, K. McCann, S. G. Boyes, and J. Braley, *Solvent Extraction and Ion Exchange*, 2017, **35 (7)**, 480.
(7) V. M. Adamov, V. I. Andreev, B. N. Belyaev, R. I. Lyubtsev, G. S. Markov, M. S. Polyakov, A. E. Ritari, and A. Y. Shil'nikov, *Soviet Radiochemistry (English Translation)* 1988, **29 (6)**, 775.
(8) D. Magnusson, B. Christiansen, R. Malmbeck, and J. P. Glatz, *Radiochim. Acta*, 2009, **97 (9)**, 497.
(9) C. Musikas, *Inorganica Chimica Acta*, 1987, **140**, 197-206.
(10) C. Musikas, *Separation Science and Technology*, 1988, **23 (12-13)**, 1211.
(11) L. Berthon and M. C. Charbonnel, *Ion Exchange and Solvent Extraction, A Series of Advances*, 2010, **19**, 429.
(12) J. A. Drader, N. Boubals, B. Camès, D. Guillaumont, P. Guilbaud, G. Saint-Louis, and L. Berthon, *Dalton Transactions*, 2018, **47 (1)**, 251.
(13) B. Ruikar, M. S. Nagar, and M. S. Subramanian, *Journal of Radioanalytical and Nuclear Chemistry*, 1992, **159**, 167.
(14) K. J. Parikh, P. N. Pathak, S. K. Misra, S. C. Tripathi, A. Dakshinamoorthy, and V. K. Manchanda, *Solvent Extraction and Ion Exchange*, 2009, **27 (2)**, 244.
(15) P. N. Pathak, D. R. Prabhu, A. S. Kanekar, and V. K. Manchanda, *IOP Conference Series: Materials Science and Engineering* 2010, **9 (1)**, 012082.
(16) J. F. Wishart, A. R. Cook, and J. R. Miller, *Review of Scientific Instruments*, 2004, **75 (11)**, 4359.
(17) H. Fricke and E. J. Hart, *J. Chem. Phys.*, 1935, **3**, 60.
(18) Spinks, J. W. T.; Woods, R. J. An Introduction to Radiation Chemistry; Third Edition; Wiley-Interscience: New York, 1990.
(19) S. P. Mezyk, B. J. Mincher, S. B. Dhiman, B. Layne, and J. F. Wishart, *Journal of Radioanalytical and Nuclear Chemistry* 2016, **307 (3)**, 2445.
(20) Y. Yoshida, T. Ueda, T. Kobayashi, H. Shibata, and S. Tagawa, *Nuclear Instruments and Methods in Physics Research Section A: Accelerators, Spectrometers, Detectors and Associated Equipment*, 1993, **327 (1)**, 41.
(21) A. J. Swallow and M. Inokuti, *International Journal of Radiation Applications and Instrumentation. Part C. Radiation Physics and Chemistry*, 1988, ***32*** **(2)**, 185.
(22) G. V. Buxton, C. L. Greenstock, W. P. Helman, and A. B. Ross, *Journal of Physical and Chemical Reference Data*, 1988, **17 (2)**, 513.
(23) P. Y. Jiang, Y. Katsumura, K. Ishigure, and Y. Yoshida, *Inorganic Chemistry*, 1992, **31 (24)**, 5135.
(24) S. P. Mezyk, T. D. Cullen, K. A. Rickman, and B. J. Mincher, *International Journal of Chemical Kinetics*, 2017, **49 (9)**, 635.
(25) S. M. Pimblott and J. A. LaVerne, *The Journal of Physical Chemistry A*, 1998, **102 (17)**, 2967.
(26) Z. B. Alfassi, *The Chemistry of Free Radicals: Pyroxyl Radicals*. Wiley: Chichester, West Sussex, England, 1997, ISBN: 978-0-471-97065-1.
(27) N. Condamines and C. Musikas, *Solvent Extraction and Ion Exchange*, 1988, **6 (6)**, 1007-1034.
(28) C. Dejugnat, L. Berthon, V. Dubois, Y. Meridiano, S. Dourdain, D. Guillaumont, S. Pellet-Rostaing, and T. Zemb, *Solvent Extraction and Ion Exchange*, 2014, **32**, 601-619.

(29) L. Berthon and M. C. Charbonnel, *Ion Exchange and Solvent Extraction A Series of Advances*, 2010, **19**, 429-513.
(30) V. K. Manchanda and P. N. Pathak, *Separation and Purification Technology*, 2004, **35**, 85-103.
(31) E. A. Mowafy, *Journal of Radioanalytical and Nuclear Chemistry*, 2004, **260**, 179-187.
(32) B. J. Mincher, S. P. Mezyk, G. Elias, G. S. Groenewold, C. L. Riddle, and L. G. Olson, *Solvent Extraction and Ion Exchange*, 2013, **31 (7)**, 715.
(33) K. L. Nash, R. C. Gatrone, G. A. Clark, P. G. Rickert, and E. P. Horwitz, *Separation Science and Technology*, 1988, **23 (12-13)**, 1355.

## Supplementary Information

# Impact of Chemical Environment on the Radiation Chemistry of *Di*-2-ethylhexylbutyramide (DEHBA) and Plutonium Retention

Gregory P. Horne, Christopher A. Zarzana, Travis S. Grimes, Cathy Rae, Joakim Ceder, Stephen P. Mezyk, Bruce J. Mincher, Marie-Christine Charbonnel, Philippe Guilbaud, George Saint-Louis, and Laurence Berthon.

### Steady-State Gamma Irradiation Figures

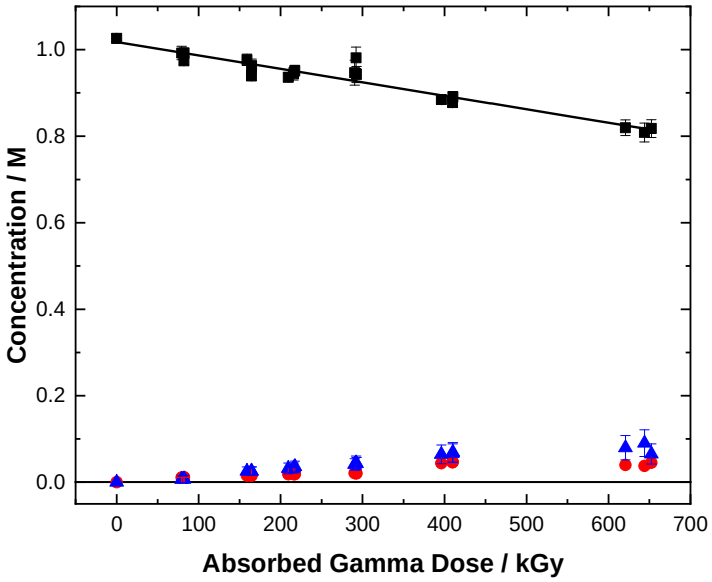


**Fig. S1** Gamma irradiation (0.82 Gy $s^{-1}$) of organic only 1.0 M DEHBA *n*-dodecane solution: DEHBA (■), MEHBA (●) and b2EHA (▲). Fitted line from linear least squares fits to data, *G*(DEHBA) = -0.31 ± 0.02 µmol $J^{-1}$.

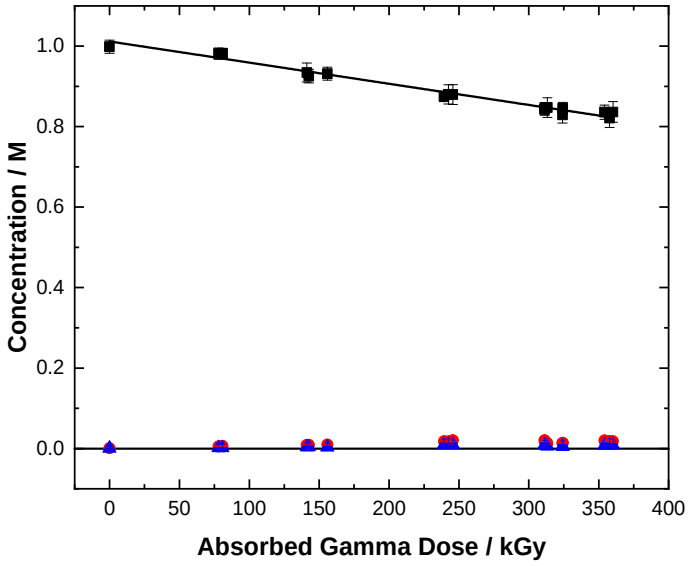


**Fig. S2** Gamma irradiation (0.82 Gy $s^{-1}$) of biphasic 0.1 M $HNO_3$ contacted 1 M DEHBA *n*-dodecane solution: DEHBA (■), MEHBA (●) and b2EHA (▲). Fitted line from linear least squares fits to data, *G*(DEHBA) = -0.53 ± 0.02 µmol $J^{-1}$.

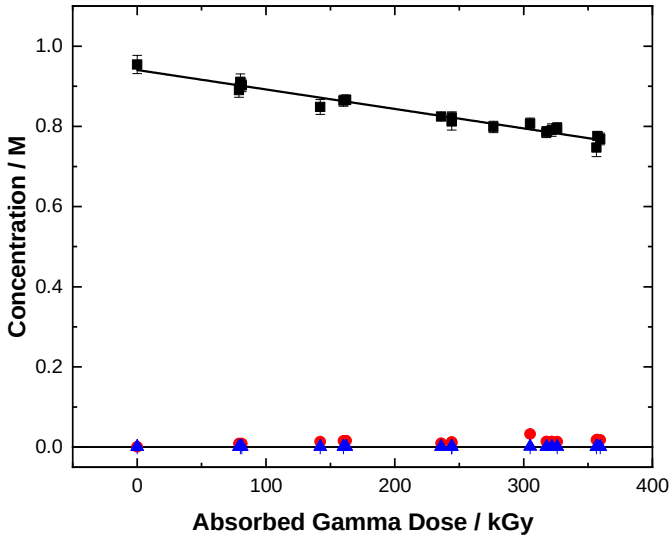


**Fig. S3** Gamma irradiation (0.82 Gy $s^{-1}$) of biphasic 3.0 M $HNO_3$ contacted 1 M DEHBA *n*-dodecane solution: DEHBA (■), MEHBA (●) and b2EHA (▲). Fitted line from linear least squares fits to data, *G*(DEHBA) = -0.49 ± 0.02 µmol $J^{-1}$.

**Reaction Kinetics**

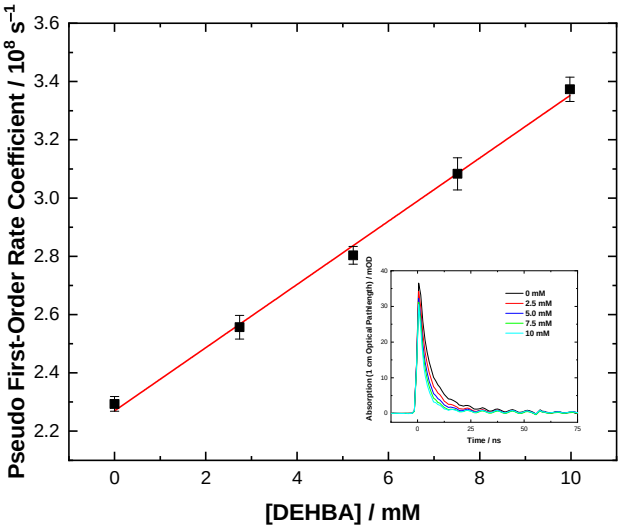


**Fig. S4** Second-order determination of the rate coefficient for the dodecane radical cation reaction with DEHBA. Solid line is a weighted linear fit, with slope corresponding to the second-order rate coefficient, $k = (1.08 \pm 0.03) \times 10^{10}$ $M^{-1}$ $s^{-1}$. *Inset:* Transient kinetic decays of the dodecane radical cation in *n*-dodecane solution containing 0.5 M dichloromethane in the presence of 0 (**Black**), 2.5 (**Red**), 5.0 (**Blue**), 7.5 (**Green**) and 10.0 (**Cyan**) mM DEHBA.

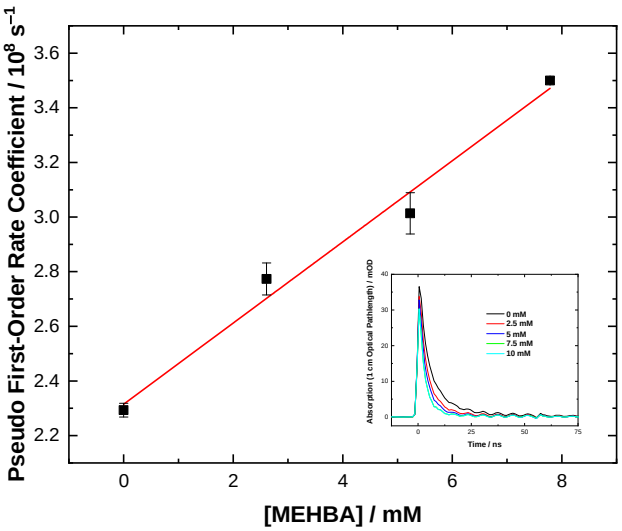


**Fig. S5** Second-order determination of the rate coefficient for the dodecane radical cation reaction with MEHBA. Solid line is a weighted linear fit, with slope corresponding to the second-order rate coefficient, $k = (1.49 \pm 0.08) \times 10^{10}$ $M^{-1}$ $s^{-1}$. *Inset:* Transient kinetic decays of the dodecane radical cation in *n*-dodecane solution containing 0.5 M dichloromethane in the presence of 0 (**Black**), 2.5 (**Red**), 5.0 (**Blue**), 7.5 (**Green**) and 10.0 (**Cyan**) mM MEHBA.

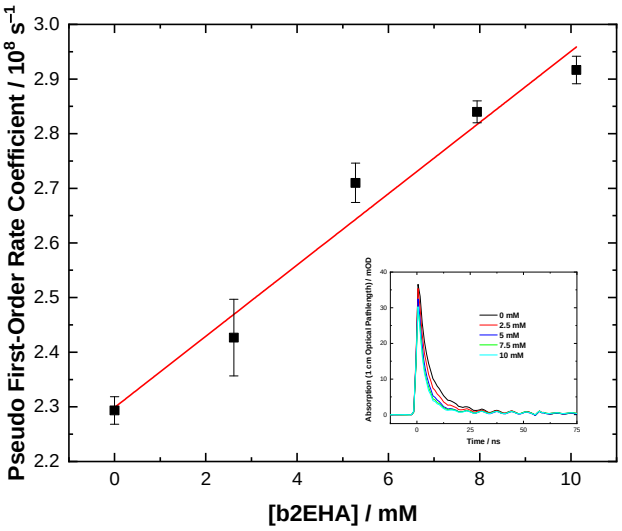


**Fig. S6** Second-order determination of the rate coefficient for the dodecane radical cation reaction with b2EHA. Solid line is a weighted linear fit, with slope corresponding to the second-order rate coefficient, $k = (6.52 \pm 0.40) \times 10^9$ $M^{-1}$ $s^{-1}$. *Inset:* Transient kinetic decays of the dodecane radical cation in *n*-dodecane solution containing 0.5 M dichloromethane in the presence of 0 (**Black**), 2.5 (**Red**), 5.0 (**Blue**), 7.5 (**Green**) and 10.0 (**Cyan**) mM b2EHA.

**Mass Balance**

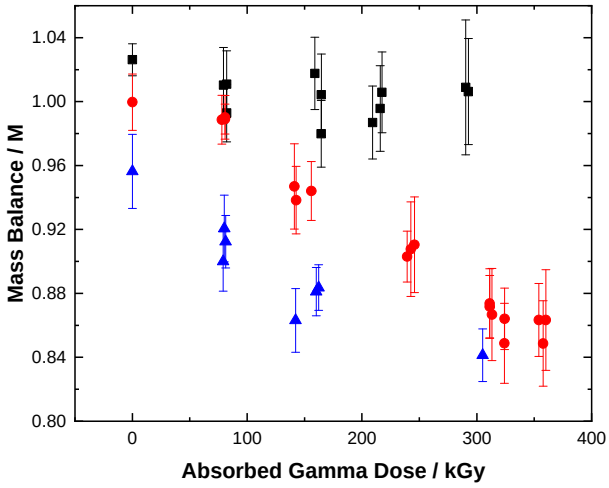


**Fig. S7** Mass balance, assuming radiolysis of a single DEHBA molecule yields either one MEHBA or one b2EHA molecule, from the gamma irradiation (0.82 Gy $s^{-1}$) of 1.0 M DEHBA *n*-dodecane solution: organic only (■), and biphasic contact with 0.1 (●) and 3.0 (▲) M $HNO_3$.

**Mass Spectrometer Parameters**

**Source Parameters**

End Plate Offset: 500 V

Capillary: 4500 V

Nebulizer Pressure: 4.0 bar

Dry Gas flow rate: 9.0 L $min^{-1}$

Dry Gas temperature: 220 °C

Mass Range: 40-800 *m/z*

**Tune Parameters**

Funnel 1 RF: 200 Vpp

Funnel 2 RF: 200 Vpp

IsCID Energy: 0.0 eV

Hexapole RF: 121.4 Vpp

Quadrupole Ion Energy: 4.0 eV

Low Mass Cutoff: 40.00 *m/z*

Collision Energy: 8.0 eV

Collision RF: 227.8 Vpp

Transfer Time: 80.8 µs

Pre-Pulse Storage Time: 5.0 µs

**Mass Calibration**

The tune mixture was composed of formic acid (Fisher Optima) and 1 M sodium hydroxide (Fisher, prepared in Fisher Optima LC/MS grade water) diluted in 50/50 water/2-propanol with a volume ratio of 1:5:100 (formic acid:1 M NaOH:50/50 water/2-propanol). The tuning mix was infused from 0.1 – 0.3 minutes and from 9.0 – 10.0 minutes in the run. Mass calibration was preformed using Bruker Data Analysis software using Automatic Internal Calibration the data at 9.5 – 10 minutes with the HPC calibration algorithm. The mass accuracy of the tune mix peaks infused from 0.1 – 0.3 minutes are used to verify the stability of the mass calibration throughout the run.

**Degradation Product Analysis**

**Table S1.** Compounds observed in the organic phase as a function of experimental conditions. 'L' stands for DEHBA.

| m/z | Formula | Unirradiated | 0.1 M $HNO_3$ | 4.0 M $HNO_3$ |
|---|---|---|---|---|
| 130.1 | $[C_8H_{17}NH_2]\ H^+$ | | | * |
| 171.1 | Contaminant | * | | |
| **200.2** | **$[C_{12}H_{24}NO]H^+$ (MEHBA)** | * | * | * |
| **242.2** | **$[C_{16}H_{35}N]\ H^+$ (b2EHA)** | | * | * |
| **256.2** | **$[C_{16}H_{33}NO]H^+$** | * | * | |
| 270.2 | $[C_{16}H_{31}NO_2]H^+$ | | * | |
| **310.2** | **$[C_{20}H_{39}NO]H^+$** | | * | * |
| **312.2** | **LH+ (DEHBA)** | * | * | * |
| **326.0** | **$[C_{20}H_{39}NOO]H^+$** | | | * |
| 328.0 | $[C_{20}H_{40}NOOH]H^+$ | | | * |
| 334.2 | $LNa^+$ | | | * |
| 350.0 | $LK^+$ | | | * |
| 357.3 | **$[C_{20}H_{40}N_2O_3]H^+$** (+NO2) | | | * |
| 354.3 | Contaminant | * | * | * |
| 368.3 | | | * | |
| 379.2 | | | | * |
| 382.3 | | | * | |
| 410.5 | $[C_{28}H_{59}N]H^+$ | | * | |
| 422.4 | | | * | |
| 447.3 | | * | | |
| 480.5 | $[C_{32}H_{65}NO]H^+$ | | * | |
| 533.5 | | | * | * |
| 551.7 | $[C_{36}H_{74}N_2O]H^+$ | | * | |
| 553.6 | $[(C_{20}H_{41}NO)(C_{16}H_{35}N)]H^+$ **(adduct)** | | | * |
| 621.6 | $[C_{40}H_{80}N_2O_2]H^+$ | | * | |
| 623.6 | $L_2H^+$ | * | * | * |
| 645.5 | $L_2Na^+$ | * | * | * |
| 661.1 | $L_2K^+$ | | | * |

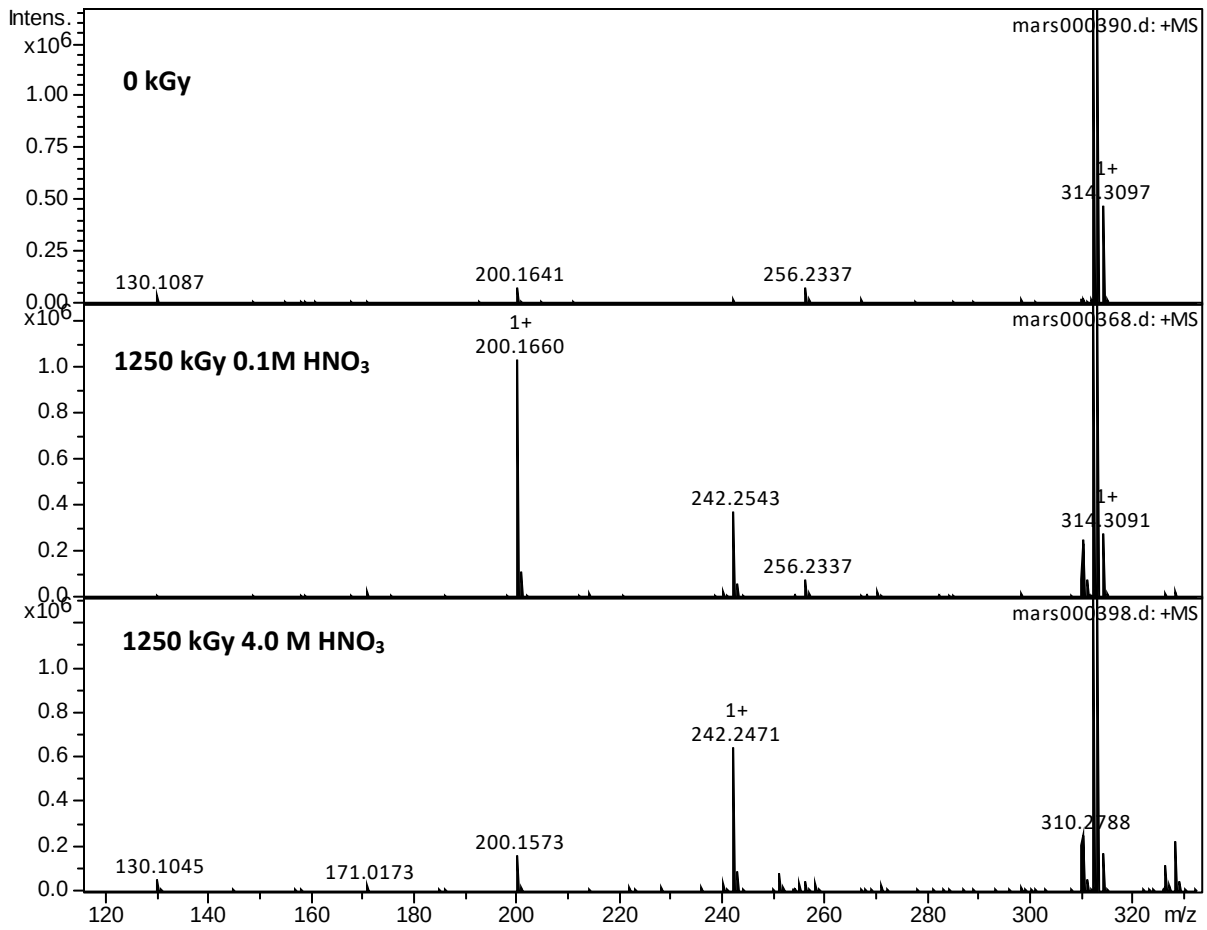


**Fig. S8.** ESI-MS spectra of organic phases of 1.0 M DEHBA *n*-dodecane solution before and after irradiation (1.25 MGy) in contact with either 0.1 or 4.0 M $HNO_3$. *In order to detect the minor peaks, the intensity of the peak corresponding to DEHBA is cut.*

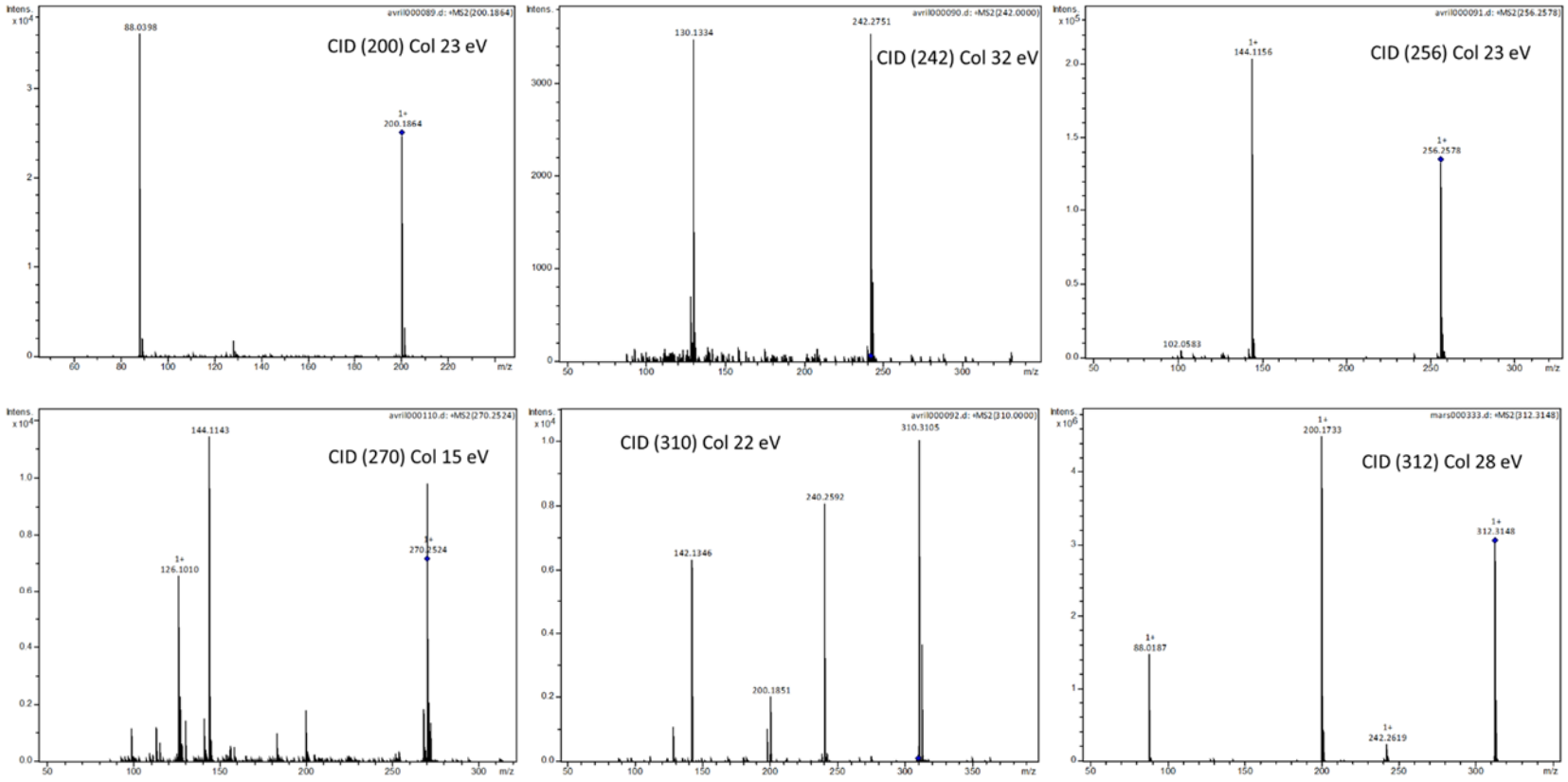


**Fig. S9** CID spectra for the main ions at 200, 242, 256, 270, 310, and 312.

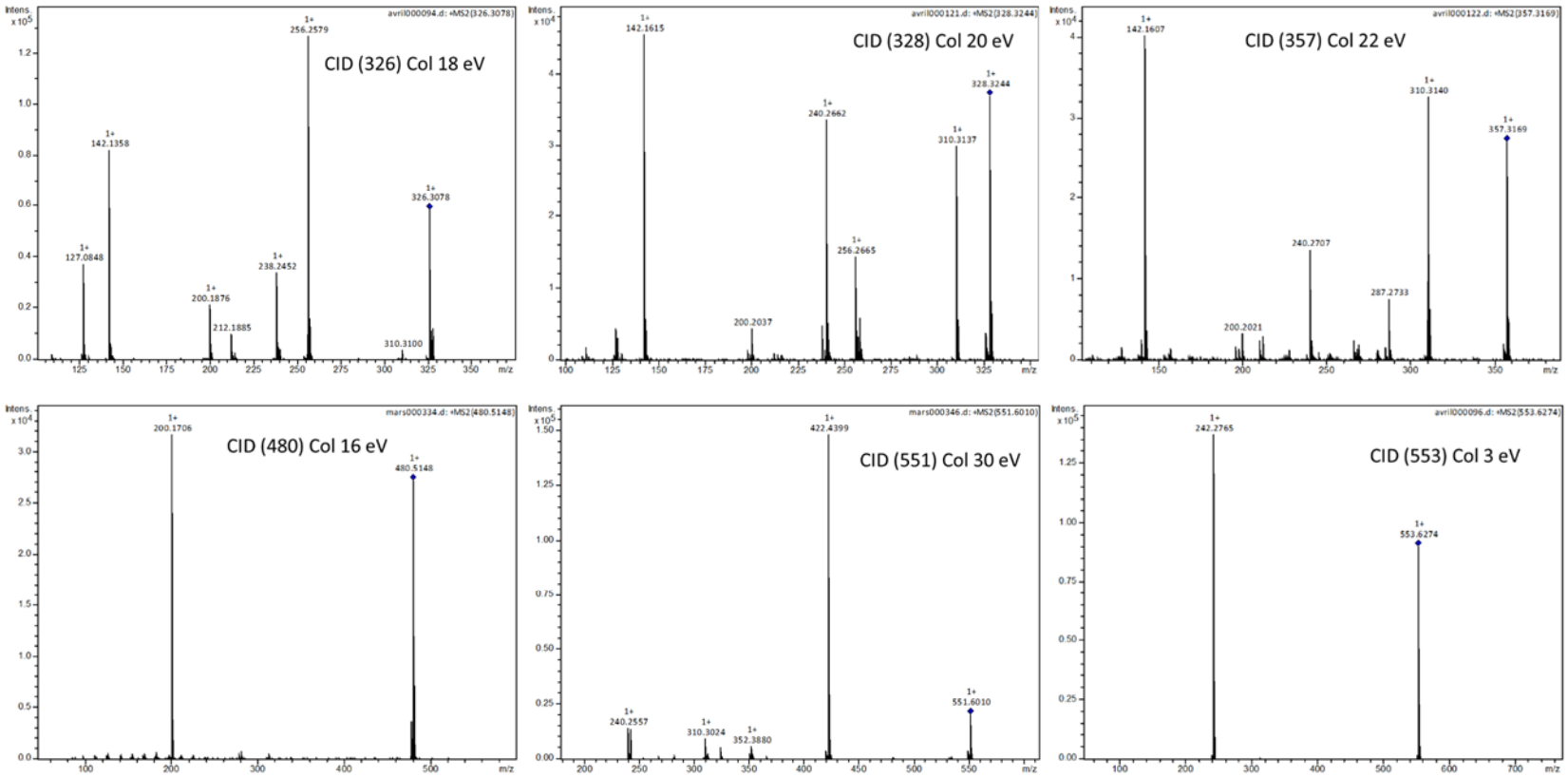


**Fig. S10** CID spectra for the main ions at 326, 328, 357, 480, 551, and 553.

**Degradation Schemes**

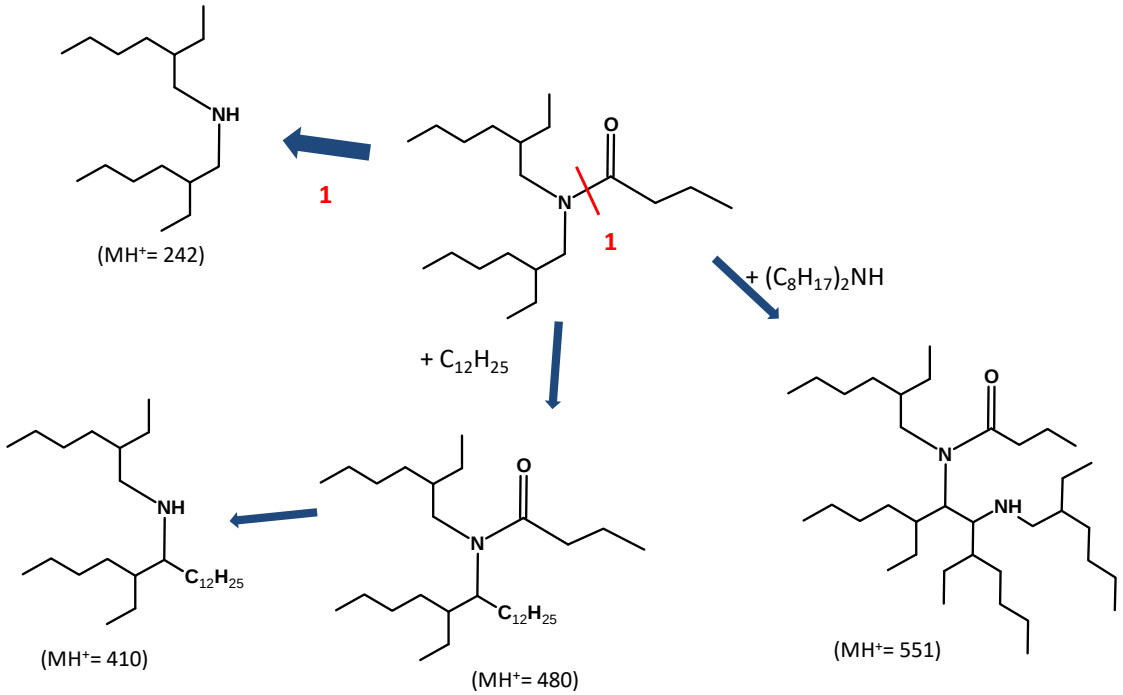


**Fig. S11** Proposed radiation-induced DEHBA degradation pathways in the presence of low 0.1 M $HNO_3$, informed by degradation product analysis.

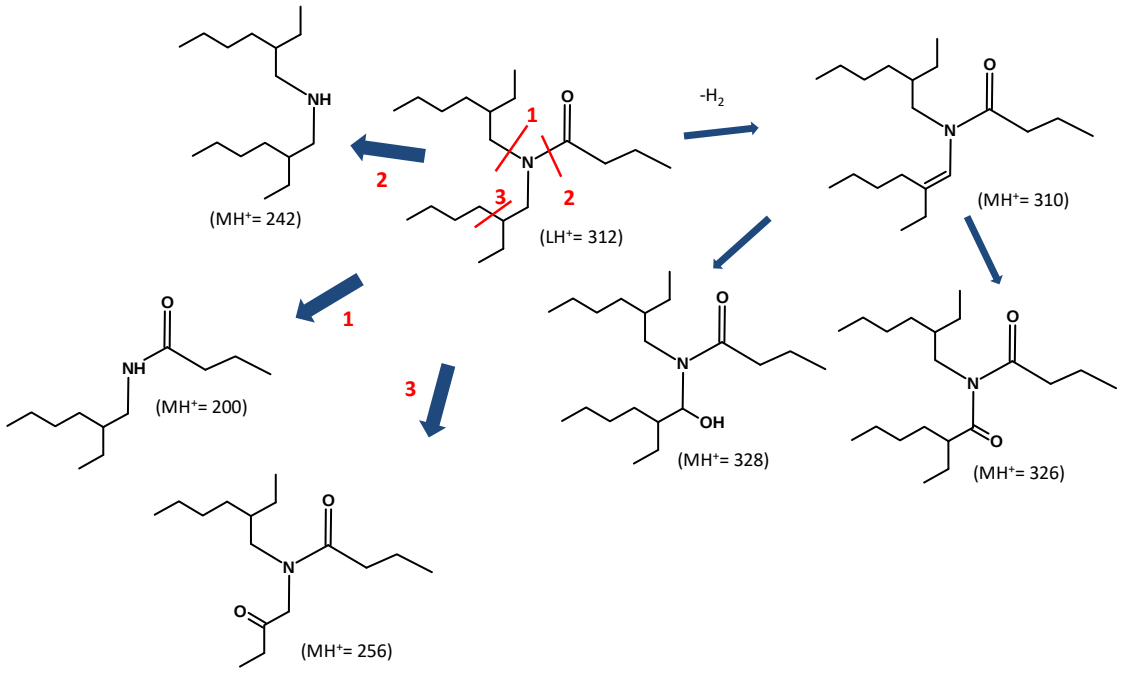


**Fig. S12** Proposed radiation-induced DEHBA degradation pathways in the presence of 3.0 $HNO_3$, informed by degradation product analysis.

**Colour Development**

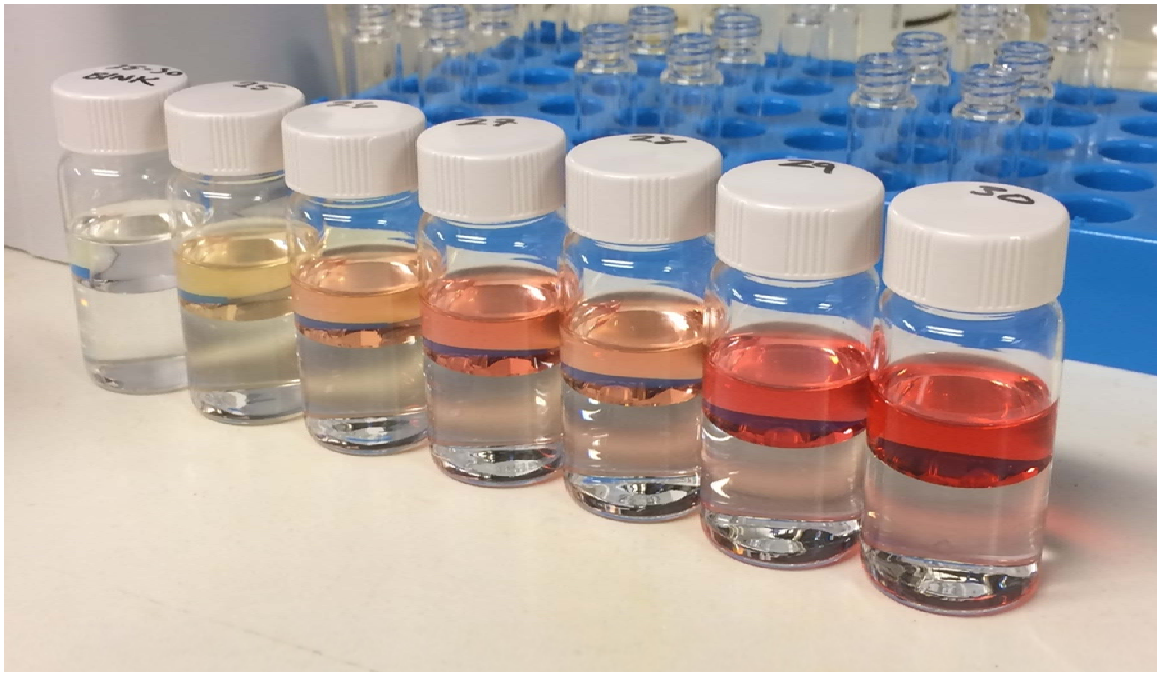

**Fig. S13** Colour change of gamma irradiated organic-only 1.0 M DEHBA *n*-dodecane solution following contact with 4.0 M $HNO_3$ (extraction conditions). *From left to right:* 0, 81, 163, 214, 292, 405, and 639 kGy.